RSC Advances

PAPER

View Article Online
View Journal | View Issue

Cite this: *RSC Adv.*, 2024, **14**, 3314

Functionalized graphene-based materials for cementitious applications†

Andrea Cacciatore,[ab] Paolo Zardi,‡[b] Laura Capone[a] and Michele Maggini *[bc]

Graphene-based materials (GBM) are promising cementitious composite additives that can significantly improve the mechanical characteristics and durability of concrete due to their unique properties, such as high surface area and aspect ratio and excellent tensile strength, to name a few. To display their full potential, GBM have to be homogeneously dispersed into the aqueous environment of cement-based matrices. The present study addresses the issue of limited dispersibility in the aqueous media of GBM through the chemical functionalization of mono- and few-layer graphene structures with hydrophilic aryl sulfonate groups and shows that a series of mortar samples containing modified GBM exhibit increased flexural and compressive strength by up to 17% and 30%, respectively, compared to mortar references without additives.

Received 10th October 2023
Accepted 16th January 2024

DOI: 10.1039/d3ra06886b

rsc.li/rsc-advances

1 Introduction

Cement composite materials (CCM), including paste, mortar, and concrete, are the most widely used and available construction materials.[1] However, CCM exhibit significant drawbacks related to their low tensile strength and brittle nature, making concrete vulnerable to cracking and degradation.[2] Therefore, intensive efforts are still underway to improve the mechanical properties and durability of CCM. Reducing concrete consumption is also relevant from a sustainability point of view; in fact, cement production is an energy intensive process that accounts for around 8% of global CO_2 emissions.[3,4] Several reported studies address these problems by adding specific binders or nano additives, such as nanostructured oxides or carbon-based materials, to increase the compressive and tensile strengths of CCM.[5–8] The addition of carbon nanomaterials, such as carbon nanotubes (CNT) or graphene-based materials (GBM), has gained increasing interest in improving the properties of cementitious materials due to their unique mechanical, thermal, and electrical characteristics.[9] The incorporation of CNT improves both mechanical and resilience properties, compared to reference samples without CNT, by reducing the porosity of CCM as a consequence of a pore filling effect.[10,11] Similarly, graphene oxide (GO) was extensively studied and found to act as a filler in the cement matrix or as a promoter, during the hydration process, of more nucleation sites leading to smaller and well-distributed pores, which are beneficial for the mechanical and durability performance of the final composite material.[12,13] In addition to GO, few-layer graphenes (FLG) are also promising materials to improve the flexural/compressive strength and durability of CCM, since the graphene carbon planes act as nano nucleation points to provide a more compact and uniform microstructure.[14] Furthermore, the use of FLG in cement improves the electrical and self-sensing properties for the production of "smart" concrete.[15]

Several reports demonstrate that the addition of a small amount of GBM (less than or equal to 0.05% by weight of cement) can effectively increase the flexural/compressive strength of CCM.[16–18] However, GBM can express their full potential if they are uniformly dispersed in the cementitious matrix. This is a challenging task due to the hydrophobic nature of the graphene core and its tendency to aggregation.[19] Even in the case of water-soluble GO and functionalized GO additives, the high concentration of Ca^{2+} ions, involved in the cement hydration process, can cause agglomeration[20] leading to partial dispersion of GO and therefore limited improvement and reproducibility of the mechanical properties of the CCM.[21] This is why, in the present study, we focus on GBM based on functionalized single-layer graphene (SLG)/FLG and not on GO or functionalized GO.

A convenient approach to improve the dispersibility of carbon nanostructures in polar media is their covalent functionalization with hydrophilic moieties[8,22] that can be installed through a number of efficient reaction protocols.[23] Among them, a general and useful functionalization method is that based on diazonium chemistry through the so-called Tour

[a]*Italcementi S.p.A.-Heidelberg Materials, Via Stezzano, 87, 24126 Bergamo, Italy*
[b]*Dipartimento di Scienze Chimiche, Università di Padova, Via F. Marzolo 1, 35131 Padova, Italy*
[c]*Istituto di Chimica della Materia Condensata e di Tecnologie per l'Energia – CNR, Corso Stati Uniti 4, 35127 Padova, Italy. E-mail: michele.maggini@unipd.it*

† Electronic supplementary information (ESI) available. See DOI: https://doi.org/10.1039/d3ra06886b

‡ Present address: Dipartimento di Scienze Chimiche e Geologiche, Università di Modena e Reggio Emilia, Via G. Campi 103, 41125 Modena – Italy.

reaction.[24] Stable diazonium salts, which can be isolated earlier or generated *in situ* from a broad number of aniline precursors, undergo reductive dissociation, which, upon nitrogen extrusion, gives an aryl radical that reacts with a double bond of the carbon nanostructure. The reaction, initially developed to functionalize CNT, has also been successfully applied to prepare a wide variety of functionalized GBM.[25,26] It is a fast and versatile reaction because it enables the introduction of a variety of substituted aryl moieties, thus creating the conditions of increasing the polarity of the hydrophobic carbon core to achieve water dispersibility. In the present work, we linked the polar aryl sulfonate group by the Tour reaction onto four commercial pristine GBM samples based on SLG and FLG. To the best of our knowledge, this is the first example where such an approach is described to prepare cementitious composites containing graphene and determine whether it is advantageous in improving the mechanical properties of mortars.

2 Experimental section

2.1. Materials

The commercial pristine GBM employed in the present study are listed below along with their main features, as declared in the technical data sheets.

- GBM **1**: FLG powder (1–5 layers), with an average lateral size of up to 9 μm, and 99.9% C; supplied by Proton Power.

- GBM **2**: SLG powder, with an average lateral size of up to 5 μm, and 99.9% C; purchased from Carlo Erba.

- GBM **3**: FLG powder (6–10 layers), with an average lateral size of up to 1 μm, and more than 95% C; supplied by NanoXplore.

- GBM **4**: FLG powder (6–10 layers), with an average lateral size of up to 2 μm, and more than 91% C; supplied by NanoXplore.

The cement used was a white Roccabianca 42.5R Portland cement, type CEM II/B-LL 42.5 R, that was supplied by Italcementi S.p.A., while the Creactive-IVK superplasticizer (**SP**), a specific admixture for mortars based on polycarboxylate ether polymers, was produced by Sika Italia S.p.A. Aniline-4-sulfonic acid and isopentyl nitrite were purchased from Sigma Aldrich and used as received.

2.2. GBM functionalization – general procedure

In a typical experiment, 500 mg of pristine GBM (41.7 mmol of C) and 120 ml of water were poured into a round-bottomed flask and treated for 10 min in an ultrasonic bath. To this suspension, an aqueous solution of the sodium salt of aniline-4-sulfonic acid, obtained by dissolving the acid (1.44 g, 8.3 mmol) in 30 ml of water containing 332 mg (8.3 mmol) of NaOH, was added and the mixture was degassed by gently bubbling nitrogen, and heated to 80 °C. After 15 min, isopentyl nitrite (1.12 ml, 8.3 mmol) was added and the suspension was stirred at 80 °C in a nitrogen atmosphere overnight. Then, the functionalized GBM was filtered on a polycarbonate membrane (Millipore Isopore VCTP, 0.1 μm porosity), and the residue washed with methanol (1 × 100 ml), and then with water (1 × 100 ml) to obtain a colourless filtrate. The solid was dried in air and then at 40 °C for 2 h in an oven. For practical reasons, the functionalization of SLG Carlo Erba pristine GBM **2** was carried out on two aliquots of 250 mg each, using half of the solvents and reagents described above for each experiment. Functionalized GBM: **1-f**, 497 mg; **2-f** 620 mg; **3-f**, 490 mg; **4-f**, 493 mg. The functionalization degree FD (also referred to as functional group coverage) of functionalized GBM was evaluated by TGA analysis as the ratio between the moles of carbon atoms (n_C) and the moles of attached aryl sulfonate groups (n_{FG}).

$$FD = \frac{n_C}{n_{FG}}$$

In particular, n_{FG} was determined from the weight loss attributed to the functional groups decomposition (between 100–650 °C). The moles of carbon (n_C) were obtained from the residual weight at 650 °C (which was the decomposition temperature of the single layer GBM **2**):

$$n_{FG} = \frac{W_{100\ ^\circ C} - W_{650\ ^\circ C}}{MW_{FG}}$$

$$n_C = \frac{W_{650\ ^\circ C}}{MW_C}$$

%FD of GBM: **1-f**, 0.05; **2-f** 1.5; **3-f**, 0.2; **4-f**, 0.07.

2.3. GBM characterization

Scanning electron microscopy (SEM) images were obtained on a field emission scanning electron microscope (Zeiss EVO MA15). Thermogravimetric analysis (Q5000IR – TA Instruments) was performed keeping the sample at 100 °C for 10 min and subsequently heating it to 900 °C with a 10 °C min^{-1} ramp in air or N_2. UV-vis spectra were recorded on an Agilent Cary 50 instrument in the 200–800 nm range with 1 cm quartz cuvettes. Samples for UV-vis analysis were prepared by suspending 10 mg of GBM in 7.0 ml of distilled water. The suspension was sonicated for 2 min using a tip sonicator (Misonix S3000) with the following pulse parameters: time on = 3 s, time off = 3 s, power level = 2 (4–6 watt) and subsequent centrifugation (Thermo Electron Corporation IEC CL 10 centrifuge) at 3500 rpm for 5 min. 100 μl (for **2-f**) or 1.0 ml (for **1-f**, **3-f** and **4-f**) of the supernatant, after centrifugation, were diluted in 3 ml of distilled water and analyzed. For stability checking of functionalized GBM in the alkaline cement environment, the aliquot of the supernatant dispersion was diluted with a saturated aqueous $Ca(OH)_2$ solution (pH = 12.5) and with a simulated cement pore solution (pH = 12.6, see Table 1).

2.4. Mortar samples preparation

Mortar samples were prepared following the European Regulation EN 196-1:2016. Two different procedures were followed before the mortar preparation to incorporate the nanostructured carbon additive when required:

- *Method A* – dry premixed binder: GBM were mixed for 20 min with cement, using a powder blender mixer.

Table 1 Composition of the simulated cement pore solution[27]

SCS component	Concentration ($g\ L^{-1}$)
$Ca(OH)_2$	Saturated
$CaSO_4$	27.6
NaOH	8.2
KOH	22.4

- *Method B* – wet sonicated solution: GBM were sonicated for 20 min in water with a superplasticizer (**SP**), using the tip sonicator described earlier.

All samples were prepared by mixing, with a Hobart mixer, the cementitious binder (containing GBM when *Method A* was followed), sand, water (containing GBM and **SP** when *Method B* was followed) using the compositions reported in Table 2. The percentage of **SP** between 0.1–0.5% by weight of cement to disperse GBM and improve cement workability was based on data from the literature.[28] Fresh cementitious mixtures were placed in rectangle molds (40 mm × 40 mm × 160 mm) and kept at 20 ± 1 °C and a relative humidity of 90 ± 15% for 24 hours; then they were demolded and submerged in a tank of water for curing (7 or 28 days).

2.5. Characterization of mortar samples

The mechanical performances of the mortar samples were evaluated according to the European Regulation EN 196-1:2016. Flexural and compressive strength were measured after 7 and 28 days of curing time in water using a compression-flexure cement test fame (Controls 65-L18Z10). The mortar samples were removed from the water and left to stand at room temperature for 20 minutes prior to mechanical investigations. To verify the reproducibility of the results, three mortar samples were prepared for each measurement.

3 Results and discussion

3.1. Functionalization and characterization of GBM

Functionalized GBM were obtained by reacting a water suspension of a pristine GBM sample with the diazonium salt of the sodium salt of aniline-4-sulfonic acid, generated *in situ* by diazotization with isopentyl nitrite (Fig. 1). Initially, the pristine GBM floated in water. The mixture then becomes a suspension as the reaction gradually progresses. SEM analyses of functionalized GBM do not reveal any significant differences from the corresponding pristine GBM, confirming that covalent functionalization does not notably affect the morphology of the samples.

Analysis of single-layer graphene samples **2** and **2-f** (Fig. 2) shows the highest lateral dimension (~6 μm) and the lowest thickness, if compared to the other GBM samples, as expected.

Characterization of functionalized GBM by thermogravimetric analysis (TGA) is reported in Fig. 3. Excluding single-layer graphene samples **2** and **2-f**, all other pristine and

Table 2 Sample codes and composition of mortars

	Entry	Mortar sample code	GBM	GBM [g]	Cement [g]	Sand [g]	Water [g]	**SP**[a] [g]
Method A dry pre-mixed	1	**A1**	**1**	0.225	449.8	1350	225	—
	2	**A1-f**	**1-f**	0.225	449.8	1350	225	—
	3	**A2**	**2**	0.225	449.8	1350	225	—
	4	**A2-f**	**2-f**	0.225	449.8	1350	225	—
	5	**A3**	**3**	0.225	449.8	1350	225	—
	6	**A3-f**	**3-f**	0.225	449.8	1350	225	—
	7	**A4**	**4**	0.225	449.8	1350	225	—
	8	**A4-f**	**4-f**	0.225	449.8	1350	225	—
	9	**A0**	—	—	500.0	1350	225	—
Method B wet sonicated	10	**B1**	**1**	0.225	449.8	1350	190	1.8
	11	**B1-f**	**1-f**	0.225	449.8	1350	190	1.8
	12	**B2**	**2**	0.225	449.8	1350	190	1.8
	13	**B2-f**	**2-f**	0.225	449.8	1350	190	1.8
	14	**B3a**	**3**	0.225	449.8	1350	190	1.8
	15	**B3-fa**	**3-f**	0.225	449.8	1350	190	1.8
	16	**B3b**	**3**	0.450	449.6	1350	190	2.0
	17	**B3-fb**	**3-f**	0.450	449.6	1350	190	2.0
	18	**B3c**	**3**	2.250	447.8	1350	190	2.2
	19	**B3-fc**	**3-f**	2.250	447.8	1350	190	2.2
	20	**B4a**	**4**	0.225	449.8	1350	190	1.8
	21	**B4-fa**	**4-f**	0.225	449.8	1350	190	1.8
	22	**B4b**	**4**	0.450	449.6	1350	190	2.0
	23	**B4-fb**	**4-f**	0.450	449.6	1350	190	2.0
	24	**B4c**	**4**	2.250	447.8	1350	190	2.2
	25	**B4-fc**	**4-f**	2.250	447.8	1350	190	2.2
	26	**B0**	—	—	500.0	1350	190	1.8

[a] **SP**: superplasticizer.

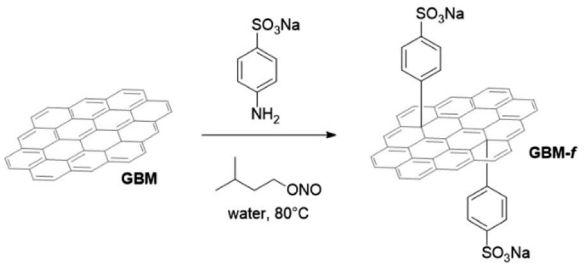

Fig. 1 Functionalization of GBM with the Tour protocol.[25,26]

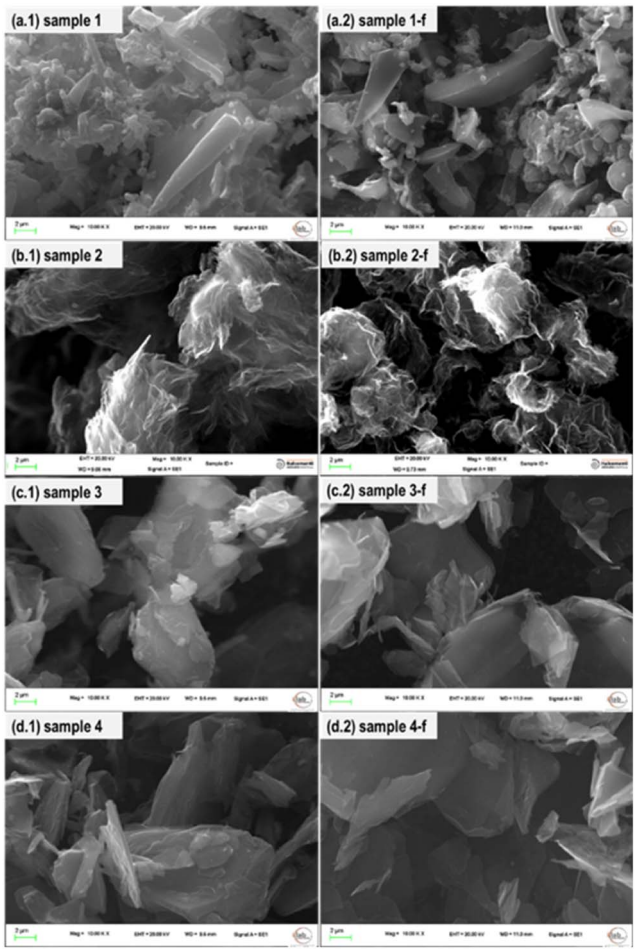

Fig. 2 SEM images of pristine (left panels) and functionalized (right panels) GBM samples.

functionalized samples show a stable TG profile up to approximately 800 °C. **2-f**, in particular, showed a 10% weight reduction compared to pristine **2**, with a peak centred at around 550 °C on the derivative weight loss curve, which is consistent with the decomposition of organic functionalities covalently linked to graphene.[29] Also, the presence of a single sharp peak points towards a uniform functionalization of the carbon lattice. A modest weight variation was recorded for samples **1-f**, **3-f**, and **4-f**, reaching a maximum weight loss of 0.6% for **3-f** relative to the corresponding pristine GBM.

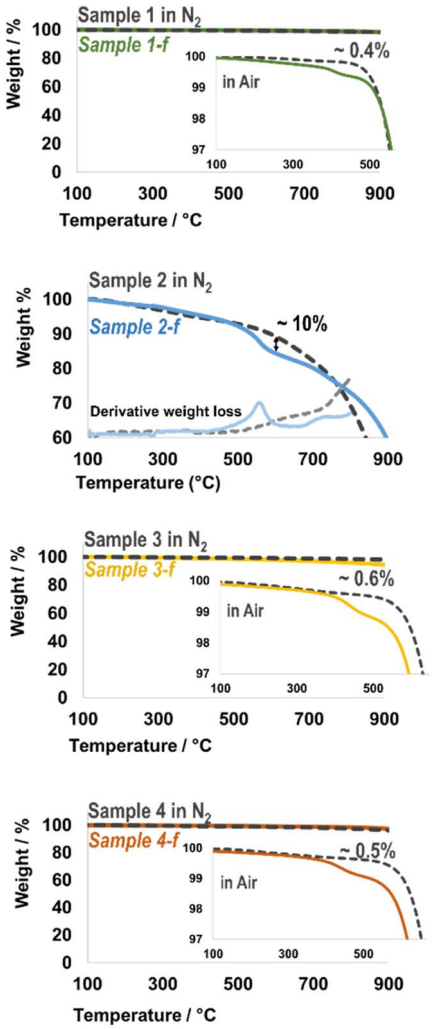

Fig. 3 Thermogravimetric analysis under nitrogen and in air for pristine and functionalized GBM.

Dispersibility in water is an important prerequisite for a successful distribution of GBM in the cement matrix. Dispersions in water of pristine and functionalized GBM aliquots (Table 2) were prepared by tip sonication, followed by centrifugation (see Section 2.3). The Fig. S1, reported in the ESI,† shows that the best dispersion of GBM in water is obtained with **2-f**, as indicated by the fully coloured liquid phase after centrifugation.

Although the functionalization improves the wettability of GBM, most of the functionalized **1-f**, **3-f**, and **4-f** samples settle at the bottom of the tube after centrifugation. This could be reasonably a consequence of the low functionalization degree of pristine **1**, **3** and **4** GBM. An aliquot of each supernatant phase after centrifugation was diluted with water for UV-vis analysis (see Section 2.3), which is shown in Fig. 4. The broad band at around 270 nm for **2-f** indicates the presence of dispersed graphene material in water.[30,31] The same absorption, although broader and much less intense, can also be observed for **1-f**, **3-f**, and **4-f** dispersions. It is worth mentioning that, for detecting the 270 nm absorption band, the supernatant dilution for these

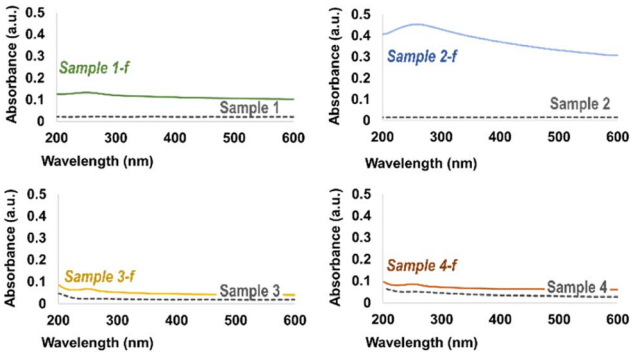

Fig. 4 UV-vis spectra of pristine and functionalized GBM.

three functionalized GBM was ten times lower than that of **2-f**. The stability of the water dispersions over time for all functionalized GBM samples was monitored every 30 min for 2 hours, and no absorbance variations were observed.

The stability of functionalized GBM in the alkaline cement environment was checked for **2-f** by diluting an aliquot of the supernatant dispersion, used for the UV-vis characterization, with a saturated aqueous $Ca(OH)_2$ solution (pH = 12.5) and with a simulated cement pore solution (pH = 12.6, see Table 1). The absorption band at 270 nm persisted for more than one hour in both cases (see Fig. S2 in the ESI†), indicating that the functionalized GBM dispersion remains substantially stable under the severe conditions of the cement hydration process.

3.2. Mortar samples with GBM

Mortar samples were first prepared using a GBM content of 0.05% by weight of cement (Table 2). Pristine and functionalized GBM were tested using two premixing methods, prior to cement hydration, during mortar preparation. *Method A* involves the dry mixing of GBM with cement. *Method B* involves the wet mixing of the GBM dispersion in water with the **SP**, which is a specific mortar admixture that allows the reduction of the water content necessary for cement hydration and improves the dispersibility of GBM additives.

The interaction between the **SP** and graphene in cement is a complex topic, with various factors, such as the type of graphene material, the specific **SP** employed, and curing conditions, capable of influencing the outcome. Our functionalized GBM, derived from pristine SLG and FLG graphene, are prone to agglomeration. The **SP** may act as a surfactant, stabilizing GBM–water suspensions, minimizing agglomeration and promoting an even distribution of graphene within the cement matrix.[32]

To better evaluate the contribution of GBM to the properties of the final mortar, two reference samples were also prepared: sample **A0** without any additive in the mortar and sample **B0** which included only the **SP**. Fig. 5a shows the flexural and compressive strength of the mortar samples prepared with *Method A* that allows better differentiation between samples containing pristine and functionalized GBM. An improvement in strength for all mortars containing GBM, with respect to **A0**, is evident after 28 days of curing. The different characteristics of functionalized GBM (that is, number of layers, morphology, degree of functionalization) should influence the final properties of cementitious material.[18] However, with *Method A*, no relevant variations, in terms of improved flexural and compressive strength, were highlighted in this context. For example, sample **A2-f**, prepared using SLG, shows an increase in flexural and compressive strength of 8%. Similarly, sample **A3-f**, prepared using FLG, improved by 6–8% both mechanical strengths. The best results were obtained with **A1-f**, showing an increase in flexural and compressive strength of 11% and 9%, respectively.

The impact of GBM functionalization could be observed also for mortars prepared with *Method B* (Fig. 5b). All samples containing functionalized GBM show mechanical strength values higher than those recorded with pristine GBM, although to a lesser extent than those recorded with *Method A*. Probably, the presence of the **SP** somehow flattens the contribution given by the functionalization to the dispersibility of GBM in the mortars. Sample **B2-f**, prepared from SLG, shows the highest flexural and compressive strength after 28 days of curing, with an increase of 17% and 30% and of 8% and 12% compared to reference samples **A0** and **B0** respectively. Using *Method B*, the different GBM characteristics have a higher impact on the final mechanic properties. It is reasonable to assume that the **SP** additive helps to a greater extent the dispersion of the functionalized SLG additive **B2-f** in the mortar, compared to the other functionalized GBM prepared from FLG.

In most cases, a GBM content higher than 0.05% by weight of cement does not have additional benefits on the mechanical properties of the final mortars.[17] However, there is increasing interest in the production of self-sensing concrete,[15] which is an attractive smart material for real-time monitoring of the status of a building. In this connection, the electrical properties of GBM[9] can be used, at least in principle, for the non-invasive detection of stress areas and cracks in the concrete structure.

This application requires a content of GBM additive higher than the 0.05% w/w considered above.[33] To investigate the feasibility of this approach and the potential impact of a higher dose of functionalized GBM on the mechanical properties of the final concrete, we prepared a series of mortar samples with *Method B* having a GBM content of up to 0.5%. We selected GBM **3-f** and **4-f** because they confer concrete mechanical characteristics that are comparable to those given by the more expensive **1-f** and **2-f**. Additionally, the **SP** loading was varied according to the GBM content to achieve the same workability for all mortars, as reported in entries 15–26 of Table 2. A picture of the mortar samples is shown in the ESI.†

The mechanical strengths of the mortar samples generally worsen with a high dose of pristine GBM.[34] For instance, the mortar samples containing 0.05%, 0.1%, and 0.5% of pristine GBM **4** show decreasing compressive strengths (57.3, 51.8, and 53.9 MPa, respectively) by increasing the GBM content (see Fig. 5c). On the contrary, excluding the flexural strength values for samples containing **4-f**, all mortars containing functionalized GBM showed mechanical performances higher than those of mortars containing pristine materials and less influenced by

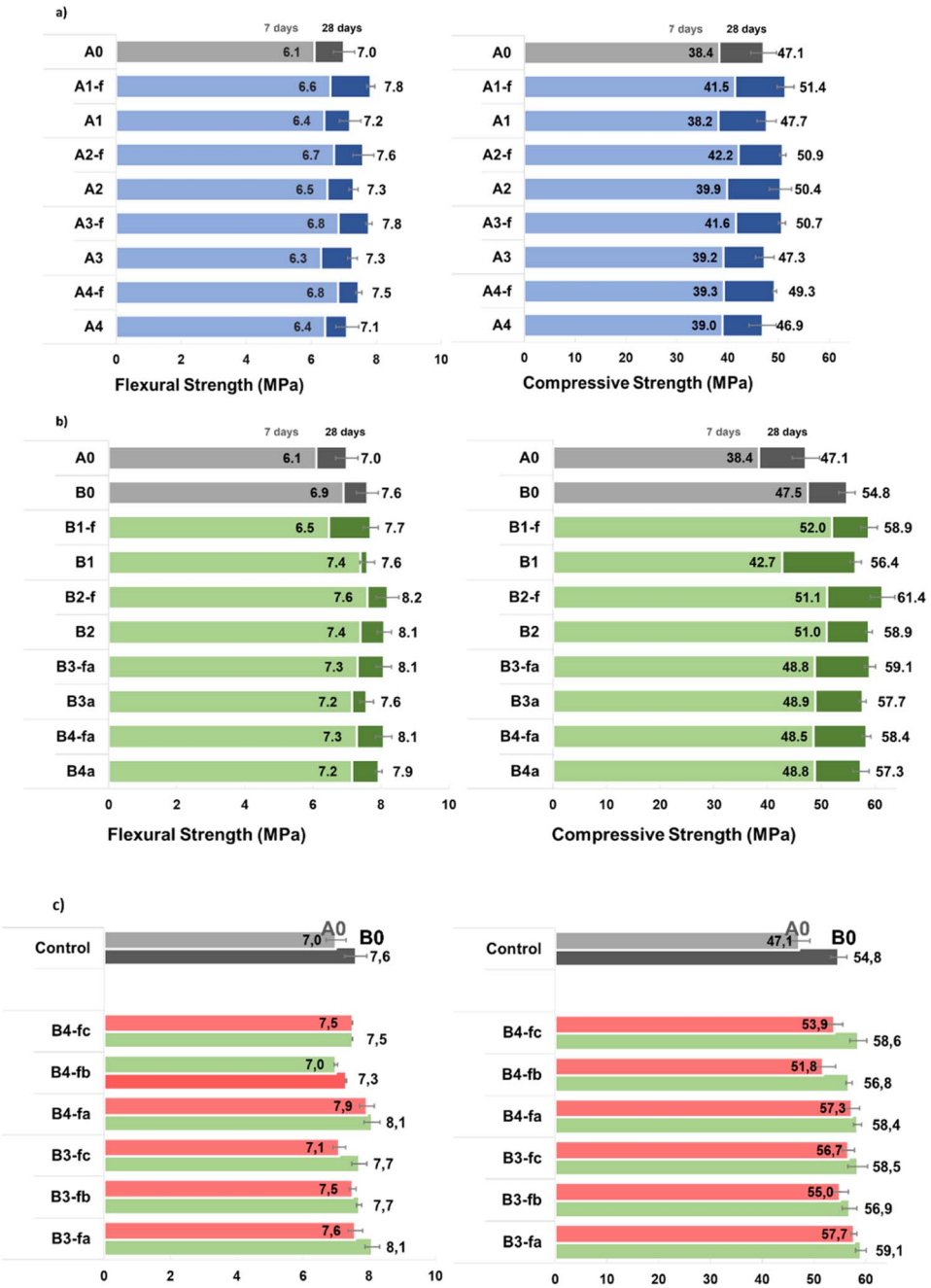

Fig. 5 Flexural and compressive strength values of mortar samples prepared with (a) 0.05% of GBM by weight of cement using *Method A* and measured after 7 and 28 days of curing; (b) 0.05% of GBM by weight of cement using *Method B* and measured after 7 and 28 days of curing; (c) 0.05–0.5% of GBM by weight of cement using *Method B* and measured after 28 curing days; the red bars refer to the mechanical performance of mortars containing pristine GBM **3** and **4**, the green bars represent the performance of mortars containing functionalized GBM **3-f** and **4-f**. GBM content is highlighted in the final letter of the mortar code *a* = 0.05 w/w, *b* = 0.1% w/w, *c* = 0.5% w/w.

increasing dosage. For instance, the mortar samples containing 0.05%, 0.1%, and 0.5% of **4-f** reached compressive strength values of 58.4, 56.8 and 58.6 MPa, respectively (see Fig. 5c). Generally, at high GBM doses, the positive contribution to the mechanical strengths given by organic functionalization is more evident (up to 9% increase with respect to the sample containing the corresponding pristine material).

4 Conclusions

The aim of this study was to understand whether functionalized GBM, not derived from GO, could offer advantages in improving the mechanical properties of cement. To this end, we decorated four commercial GBM (pristine SLG and FLG samples) with phenyl sulfonate groups to improve their dispersion in water and, possibly, in cement composites. Although a significant

degree of functionalization was obtained only from SLG, an improvement in water dispersibility was also observed for functionalized FLG **1-f**, **3-f**, and **4-f**. The addition of functionalized SLG and FLG to mortar samples led to better mechanical performance. The best results were obtained using functionalized SLG **2-f** and a **SP**, with an increase in flexural and compressive strength of 17% and 30%, compared to mortar samples without GBM additives.

Interestingly, the use of less functionalized, but less expensive, **3-f** and **4-f** was also effective, although to a slightly lower extent than **2-f**, for the preparation of cement composites with a high dose of GBM. Despite the detrimental effect of a GBM content greater than 0.05% (by weight of cement) which is generally observed, the composite mortar samples preserved the mechanical properties observed with a lower GBM content, as a consequence of the functionalization of the GBM additive.

This observation opens the door to further studies on cementitious composites, wherein electrical or thermal conductivity can be enhanced by incorporating higher doses of functionalized GBM derived from commercial single-layer and few-layer graphene.

Conflicts of interest

There are no conflicts to declare.

References

1 G. Habert, S. A. Miller, V. M. John, J. L. Provis, A. Favier, A. Horvath and K. L. Scrivener, *Nat. Rev. Earth Environ.*, 2020, **1**, 559–573.
2 D. W. Hobbs, *Int. Mater. Rev.*, 2001, **46**, 117–144.
3 S. A. Miller, A. Horvath and P. J. M. Monteiro, *Environ. Res. Lett.*, 2016, **11**, 074029.
4 P. J. M. Monteiro, S. A. Miller and A. Horvath, *Nat. Mater.*, 2017, **16**, 698–699.
5 C. S. R. Indukuri, R. Nerella and S. R. C. Madduru, *Constr. Build. Mater.*, 2019, **229**, 116863.
6 E. Shamsaei, F. B. de Souza, X. Yao, E. Benhelal, A. Akbari and W. Duan, *Constr. Build. Mater.*, 2018, **183**, 642–660.
7 P. Feng, H. Chang, X. Liu, S. Ye, X. Shu and Q. Ran, *Mater. Des.*, 2020, **186**, 108320.
8 C. Paul, A. S. van Rooyen, G. P. A. G. van Zijl and L. F. Petrik, *Constr. Build. Mater.*, 2018, **189**, 1019–1034.
9 M. Krystek, A. Ciesielski and P. Samorì, *Adv. Funct. Mater.*, 2021, **31**, 2101887.
10 A. Carriço, J. A. Bogas, A. Hawreen and M. Guedes, *Constr. Build. Mater.*, 2018, **164**, 121–133.
11 F. Gao, W. Tian, Z. Wang and F. Wang, *Constr. Build. Mater.*, 2020, **260**, 120452.
12 C. Ruan, J. Lin, S. Chen, K. Sagoe-Crentsil and W. Duan, *ACS Appl. Nano Mater.*, 2021, **4**, 10623–10633.
13 W. Li, X. Li, S. J. Chen, Y. M. Liu, W. H. Duan and S. P. Shah, *Constr. Build. Mater.*, 2017, **136**, 506–514.
14 S. Polverino, E. M. Del Rio Castillo, A. Brencich, L. Marasco, F. Bonaccorso and R. Morbiducci, *Sustainability*, 2022, **14**, 784.
15 D. D. L. Chung, *Carbon*, 2012, **50**, 3342–3353.
16 M. Chougan, F. R. Lamastra, E. Bolli, D. Caschera, S. Kaciulis, C. Mazzuca, G. Montesperelli, S. H. Ghaffar, M. J. Al-Kheetan and A. Bianco, *Nanomaterials*, 2021, **11**, 3278.
17 M. Krystek, D. Pakulski, V. Patroniak, M. Górski, L. Szojda, A. Ciesielski and P. Samorì, *Adv. Sci.*, 2019, **6**, 1801195.
18 Q. Zheng, B. Han, X. Cui, X. Yu and J. Ou, *Nanomater. Nanotechnol.*, 2017, **7**, 1–18.
19 D. W. Johnson, B. P. Dobson and K. S. Coleman, *Curr. Opin. Colloid Interface Sci.*, 2015, **20**, 367–382.
20 X. Li, A. H. Korayem, C. Li, Y. Liu, H. He, J. G. Sanjayan and W. H. Duan, *Constr. Build. Mater.*, 2016, **123**, 327–335.
21 Z. Lu, B. Chen, C. Y. Leung, Z. Li and G. Sun, *Cem. Concr. Compos.*, 2019, **100**, 85–91.
22 Y. Si and E. T. Samulski, *Nano Lett.*, 2008, **8**, 1679–1682.
23 V. Georgakilas, J. A. Perman, J. Tucek and R. Zboril, *Chem. Rev.*, 2015, **115**, 4744–4822.
24 J. L. Bahr, J. Yang, D. V. Kosynkin, M. J. Bronikowski, R. E. Smalley and J. M. Tour, *J. Am. Chem. Soc.*, 2001, **123**, 6536–6542.
25 L. Rodríguez-Pérez, R. García, M. Á. Herranz and N. Martín, *Chem.–Eur. J.*, 2014, **20**, 7278–7286.
26 G. Schmidt, S. Gallon, S. Esnouf, J.-P. Bourgoin and P. Chenevier, *Chem.–Eur. J.*, 2009, **15**, 2101–2110.
27 P. Ghods, O. B. Isgor, G. McRae and T. Miller, *Cem. Concr. Compos.*, 2009, **31**, 2–11.
28 I. Papanikolaou, L. Ribeiro de Souza, C. Litina and A. Al-Tabbaa, *Constr. Build. Mater.*, 2021, **293**, 123543.
29 P. Salice, E. Fabris, C. Sartorio, D. Fenaroli, V. Figà, M. P. Casaletto, S. Cataldo, B. Pignataro and E. Menna, *Carbon*, 2014, **74**, 73–82.
30 J. Liu, J. Fu, Y. Yang and C. Gu, *Constr. Build. Mater.*, 2019, **199**, 1–11.
31 H. Du and S. D. Pang, *Constr. Build. Mater.*, 2018, **167**, 403–413.
32 L. Zhao, X. Guo, Y. Liu, C. Ge, L. Guo, X. Shu and J. Liu, *RSC Adv.*, 2017, **7**, 16688–16702.
33 D. Lu, L.-P. Ma, J. Zhong, J. Tong, Z. Liu, W. Ren and H.-M. Cheng, *ACS Nano*, 2023, **17**, 3587–3597.
34 F. I. Ismail, N. Shafiq, Y. M. Abbas, N. Bheel, O. Benjeddou, M. Ahmad, M. M. Sabri Sabri and E. S. Ateya, *Case Stud. Constr. Mater.*, 2022, **17**, e01676.